Talanta 120 (2014) 148–157

Contents lists available at ScienceDirect

Talanta

journal homepage: www.elsevier.com/locate/talanta

Rapid microwave assisted synthesis of graphene nanosheets/polyethyleneimine/gold nanoparticle composite and its application to the selective electrochemical determination of dopamine

Vinoth Kumar Ponnusamy [a,c], Veerappan Mani [b], Shen-Ming Chen [b], Wan-Tran Huang [c], Jen-Fon Jen [a,*]

[a] Department of Chemistry, National Chung Hsing University, Taichung City 402, Taiwan
[b] Department of Chemical Engineering and Biotechnology, National Taipei University of Technology, Taipei City 106, Taiwan
[c] Department of Business Administration, Asia University, Wu-Fong, Taichung City 413, Taiwan

ARTICLE INFO

Article history:
Received 22 September 2013
Received in revised form
1 December 2013
Accepted 2 December 2013
Available online 11 December 2013

Keywords:
Graphene nanosheets
Polyethyleneimine
Gold nanoparticles
Microwave assisted synthesis
Electrocatalysis
Dopamine
Human urine samples

ABSTRACT

In this study, a simple and fast microwave assisted chemical reduction method for the preparation of graphene nanosheet/polyethyleneimine/gold nanoparticle (GNS/PEI/AuNP) composite was developed. PEI, a cationic polymer, was used both as a non-covalent functionalizing agent for the graphene oxide nanosheets (GONSs) through electrostatic interactions in the aqueous medium and also as a stabilizing agent for the formation of AuNPs on PEI wrapped GNSs. This preparation method involves a simple mixing step followed by a simultaneous microwave assisted chemical reduction of the GONSs and gold ions. The prepared composite exhibits the dispersion of high density AuNPs which were densely decorated on the large surface area of the PEI wrapped GNS. X-ray photoelectron spectroscopy, powder X-ray diffraction, high-resolution transmission electron microscopy, field-emission scanning electron microscopy with energy dispersive X-ray spectroscopy, and thermo-gravimetric analysis, were used to characterize the properties of the resultant composite. The prepared GNS/PEI/AuNP composite film exhibited excellent electrocatalytical activity towards the selective determination of dopamine in the presence of ascorbic acid, which showed potential application in electrochemical sensors. The applicability of the presented sensor was also demonstrated for the determination of dopamine in human urine samples.

1. Introduction

Graphene nanosheet (GNS), a two-dimensional (2D) macromolecule, is a single-atom-thick sheet of hexagonally arrayed sp^2-bonded carbon atoms, exhibiting extremely high specific surface area (2600 m^2/g) [1–3]. It is well-known that carbon nanotubes (CNTs) based composite nanomaterials owing to their outstanding properties have attracted significant research attention in biomedicine, catalysts, sensors, and so on [4]. GNS possesses stable physical properties that are analogous to CNTs. Moreover, it has larger surface areas, which can be considered as an unrolled CNT [5,6]. GNSs offer extraordinary electronic, thermal, and mechanical properties and are expected to find a variety of applications such as sensors, nanocomposites, batteries, supercapacitors, and hydrogen storage [7]. As recently demonstrated, GNSs can be obtained in bulk quantities by chemical reduction of graphene oxide nanosheets (GONSs) [8–10]. However, because of Van der Waals interactions, the GNSs tend to form irreversible agglomerates and even restack to form graphite [11]. In order to obtain graphene as individual sheets, attaching some molecules or polymers onto the sheets is an approach to reduce the aggregation [3,12]. Graphene-based composite nanomaterials prepared via molecular level dispersion in polymers that have shown to improve electronic and thermal conductivity has been reported [3,13,14]. Recent progress in preparation techniques has made it possible to study the properties of GNS experimentally and have been applied to metal nanoparticles (NPs) such as Pt and Au, supported on GNS [15–17].

Nowadays, nanocomposites produced by the association of GNS with metallic NPs are expected to have promising potential applications in fields such as chemical sensors, energy storage, catalysis and hydrogen storage [16]. Another important feature of the adhesion of metal NPs to GNS is that the adhesion results in the inhibition of aggregation of the GNSs in dry state. The metal

* Corresponding author. Tel.: +886 4 22853148; fax: +886 4 22862547.
E-mail address: jfjen@dragon.nchu.edu.tw (J.-F. Jen).

0039-9140/$ - see front matter © 2013 Elsevier B.V. All rights reserved.
http://dx.doi.org/10.1016/j.talanta.2013.12.003

NPs also function as a spacer, thus increasing the distance between the GNSs, thereby making both faces of graphene accessible [17]. Most of the articles reported about the preparation of graphene/metal nanocomposites make use of organic spacers, like octadecylamine, to anchor the metallic nanoparticles to the graphene surface, or organic solvents such as tetrahydrofuran, methanol and ethylene glycol [17].

Recently, graphene functionalized with gold nanoparticles (AuNPs) reduced and/or stabilized by ionic liquid has been synthesized successfully and have shown their unique properties, such as excellent electrocatalytic activity and high stability, which creates more opportunities for applications of GNS in sensors and actuators [18]. More recently, linear polyallylamine (PAH) has been used to generate colloidal aqueous suspension of cross-linked GONS for its excellent mechanical stiffness and strength towards mechanical actuators, nano/microrobots and electromechanical systems [19]. The electrical conductivity of GONS–PAH hybrid thin film transistors, and its characterization and applicability to chemically modified graphene-based label-free DNA sensors was reported recently [20]. As with other conductive additives, variations in the electrical properties of GONS (or reduced-GONS) films hybridized with polyelectrolytes (PEs) is essential to realizing their applications [20]. In spite of the great activity currently taking place in the field of hybrid films of graphene and PEs, there has not been much insight into the study of the effect of an incorporated PE on the electrocatalytic behavior of graphene hybrid films.

As an extension of this strategy, the adsorption of cationic PE on the carboxylated surface of CNTs and the attachment of negatively charged AuNPs to the PE chains through electrostatic interactions has been reported [21]. In contrast to the above surface functionalization and polymer wrapping approaches, attachment of metal NPs to CNTs using interlinkers such as pyrene derivatives, which interact with CNTs via π–π stacking represents a simple and attractive strategy [22]. However, to date, stable dispersion of graphene/polymer/metal NP composites prepared and processed exclusively in aqueous solution without covalent functionalization of GNSs has not been reported. Polyethyleneimine (PEI) is a water-soluble amine-containing cationic PE, has been known to effectively interact with CNTs via physisorption on CNTs' sidewalls [23,24] and has been demonstrated to cause significant changes in the electrical conductance of *sem*-SWNT [23]. More recently, linear PEI has been used both as reducing agent and protecting or stabilizing agent for the preparation of gold NPs [24]. Recently, much attention is also focused on the large scale microwave assisted synthesis of metallic NPs, soluble SWCNT derivatives, exfoliation of graphite intercalation compounds and large surface area 2-D GNS [25,26]. To our knowledge, a simple synthetic route for high density attachment of AuNPs onto the sides of GNS with high NP coverage has not been reported.

Dopamine (DA) is one of the important catecholamine based neurotransmitter playing a vital role in the mammalian central nervous systems and therefore its determination is of significant importance [27]. Unfortunately, the electrochemical signal of DA often associated very close and overlaps to that of ascorbic acid (AA) and suffers from interference [28]. One of the important drawback is biological samples often contain high concentrations of AA than DA (100–1000 fold higher) and hence overcoming the interference of AA is challenging task in the electrochemical determination of DA in biological samples [29]. Bare electrodes associated with the shortcomings of poor selectivity and high overpotential pave a way to look for the modified electrodes [30]. Numerous efforts were made to prepare modified electrodes to eliminate the interference from AA and ultimately for the selective determination of DA. Some of the reported literature for the selective determination of DA in the presence of AA includes, carbon nanotubes-ionic liquid gel [31], $Fe(CN)_6^{4-}$-doped-glutaraldehyde-cross-linked poly-L-Lysine film [27], graphene [29], Poly(3,4-ethylenedioxythiophene-co-(5-amino-2-naphthalenesulfonic acid)) [28], boron-doped carbon nanotubes [32], quercetin–graphene composite [33], polypyrrole–graphene composite [34], PEDOT/Palladium composite [35], porphyrin-functionalized graphene [36], gold nanoparticles anchored multi-wall carbon nanotubes [37] and chitosan–graphene composite [38]. Recently Li and coworkers reported the preparation of graphene–Au nanoparticles nanocomposite for the selective determination of dopamine, but the DPV results shows noticeable response towards 1 mM of AA [39].

In this paper, we report the preparation of GNS/PEI/AuNP composite using a simple microwave assisted synthesis method in aqueous medium. This synthetic method involves a non-covalent functionalization of exfoliated GONSs with PEI and a simultaneous chemical reduction of GONS and $HAuCl_4$ in a one step reaction. Moreover, we also demonstrated the electrocatalytic activity of the prepared GNS/PEI/AuNP composite for the selective determination of DA in the presence of high concentration of AA. PEI wrapped GNSs (high conductivity) are good substrates to maintain the size distribution of AuNPs, which exhibits good electrocatalytic activity due to its synergistic effect of PEI wrapped GNSs and 2–4 nm sized high density AuNPs. Moreover the prepared composite could be an exciting material for its use in other electrochemical sensors.

2. Experimental

2.1. Materials and methods

Graphite powder (1–2 μm), linear polyethyleneimine of average molecular weight ~25,000 and 30% hydrogen peroxide (H_2O_2) were purchased from Alfa chemicals and used as received. Sulfuric acid (H_2SO_4), hydrochloric acid (HCl), sodium nitrate ($NaNO_3$), sodium borohydride ($NaBH_4$) and potassium permanganate ($KMnO_4$) were purchased from Merck Chemicals. Dopamine (DA) and ascorbic acid (AA) were purchased from Sigma-Aldrich and used as received. The supporting electrolyte used for the electrochemical studies was 0.05 M phosphate buffer solution (PBS) of pH 7. Prior to each electrochemical experiment, the electrolyte solutions were deoxygenated with pre-purified N_2 for 15 min unless otherwise specified.

2.2. Microwave assisted synthesis of GNS/PEI/AuNP composite

In this synthesis, GONSs was prepared from graphite via modified Hummers method [40]. 5 mg of the prepared GONSs was dispersed with 9.5 mL of 1 M PEI aqueous solution and 0.5 mL of 25 mM $HAuCl_4$ in a 25 mL round bottom glass flask under ultrasonication for 10 min. Then, the above mixture solution was placed in a modified version of the domestic microwave oven NN-L520 inverter system (2450 MHz, Panasonic, Canada) with a maximum power of 1100 W, equipped with a temperature-control condenser system (YIH DER BL-720, Taiwan) [41]. A microwave stirrer (Scienceware, Bel-Art Products, NJ, USA) was also used for stirring the mixture at 300 rpm during microwave assisted synthesis. Microwave with effective power set at 200 W for a total irradiation time of 2 min was used. After the completion of 1.30 min of microwave irradiation, 0.1 mL of 0.05 M $NaBH_4$ was added into reaction mixture in order to ensure the complete reduction of any unreduced site of GONS and $HAuCl_4$ in the PEI solution. The resulting mixture solution was then centrifuged at 4000 rpm for 15 min and washed with pure water for three times. Then, the resultant composite product was dried at room temperature for overnight.

2.3. Fabrication of GNS/PEI/AuNP composite modified electrode for the electrochemical experiments

As-prepared GNS/PEI/AuNP composite was dispersed in 0.75% nafion (1 mg mL^{-1}) with the aid of ultrasonic agitation. Prior to each electrochemical experiment, GCE surface was polished well with 0.5 μm alumina slurry using Buelher polishing pad. The polished GCE was ultrasonicated in ethanol and water for 5 min to remove the adsorbed residual alumina particles and dried at ambient conditions. 5 μL dispersion of GNS/PEI/AuNP composite (1 mg mL^{-1}) was drop casted onto the pre-cleaned GCE and dried at room temperature and used for the electrochemical experiments.

2.4. Characterization techniques

The pH of the solutions was checked by an ORION Triod pH electrode using a Standard pH meter (Radiometer PHM82, Denmark). X-ray photoelectron spectroscopy (XPS) spectra were recorded using an ULVAC-PHI, PHI 5000 VersaProbe/Scanning ESCA Microprobe with a hemispherical analyzer operated on a constant pass energy mode and non-monochromatized Al Kα X-ray radiation ($h\nu$=1486.6 eV). Data analysis was performed with the "XPS peak" program. The spectra were decomposed by least-squares fitting routine using a Gauss/Lorentz product information after subtracting Shirley background. Thermogravimetric analysis (TGA) was performed on 40 mg samples on a Thermo Scientific TGA VersaTherm TGA quartz rod microbalance. The tests were done in nitrogen (250 mL min^{-1}) from 25 to 900 °C with a 10 °C/min heating ramp. All the samples were characterized by powder X-ray diffraction (p-XRD) using a PANalytical X'Pert Pro MRD (Cu Ka λ=0.15418 nm). The morphological studies of the samples were characterized using Field-emission scanning electron microscopy (FE-SEM) using a ZEISS "ULTRA plus" (Carl Zeiss International, Germany). TEM images were taken with JEOL 2000 transmission electron microscope (operating at 200 kV) equipped with an energy dispersive X-ray (EDX) analyzer. Electrochemical measurements were carried out using a CHI 750a work station. Electrochemical studies were performed in a conventional three electrode cell using BAS GCE as a working electrode (area 0.07 cm^2), saturated Ag/AgCl as a reference electrode and Pt wire as a counter electrode. Amperometric measurements were performed with analytical rotator AFMSRX (PINE instruments, USA) with a rotating disc electrode (RDE) having working area of 0.24 cm^2.

3. Results and discussion

3.1. Fabrication of GNS/PEI/AuNP composite

A schematic representation of the preparation of GNS/PEI/AuNP (high density AuNP decorated PEI wrapped GNS) composite is shown in Fig. 1. The driving force behind the non-covalent functionalization of cationic PEI on each sheet of GONS is the electrostatic interaction between the oppositely charged GONSs and PEI along with the physisorption process, which is analogous to polymer wrapping process [21,24]. The major interaction between the polymer backbone and nanosheets surface is the most likely cation–π interactions of PEI and GONSs that extends to self-assembly [21]. It is worth mentioning that this approach allows control over the distance between functional groups on the GONSs surface through variation of the polymer backbone and side chains [19]. This approach allows the dispersion and individualization of GONSs in aqueous solution by cation–π interactions with polymer wrapping [19,20]. More importantly, it has been reported that amines possess high affinity for physisorption along

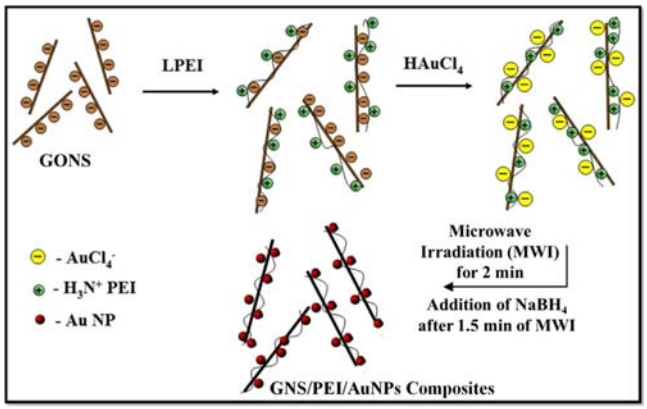

Fig. 1. Schematic illustration of the preparation of GNS/PEI/AuNP composite.

CNTs' sidewalls, which is also similar to GNS [24,42,43]. Moreover, PEI can form PEI–metal ion complex, which can adsorb easily on the surface of the GONSs via electrostatic interaction [44]. PEI has a high density of imino-groups, which can serve as primers for the adsorption of anionic $AuCl_4^-$. It also acts both as reducing agent and stabilizing agent for AuNPs and GONSs [24]. As GONS has been found to contain reactive epoxy groups, its exposure to free amine groups of PEI would lead to a ring-opening reaction of the reactive three-membered epoxide ring, creating new C–N bonds. The ring-opening reaction of the epoxy group from attack by nucleophiles such as amine groups has been well established [19]. Addition of mild amount of $NaBH_4$ to the reaction mixture facilitated reduction of any remaining unreduced GONSs sites that evaded chemical functionalization [44]. By combining the multifunction of PEI, the attachment of high density AuNPs on the surface of GNSs was achieved. This synthetic method does not need any exhaustive separate reduction reaction steps for GONS and gold ions [14,16]. High polarizability of graphene layers causes them to heat rapidly under MWI approach, which provides simple and fast routes to the synthesis of this composite [25] and since the metal precursor has large microwave absorption cross sections relative to the solvent, very high effective reaction temperatures can be achieved [25]. This allows the rapid decomposition of the precursors, thus creating highly supersaturated solutions where nucleation and growth can take place to produce the desired gold nanocrystalline product on each PEI wrapped GNS.

3.2. XPS and powder-XRD studies of GNS/PEI/AuNP composite

The formation of GNS and the non-covalent functionalization of PEI have been confirmed further by XPS, which is an effective tool to examine the evolution of functional groups on the surface of carbon-based materials [46]. Fig. 2(a) is the XPS spectrum of the GNS/PEI/AuNP composite in a wide scan. Fig. 2(b) shows the high-resolution XPS spectrum of AuNPs in the composite. The Au $4f_{7/2}$ and $4f_{5/2}$ peaks appear at ca. 83.8 and 87.4 eV (peak-to-peak distance of 3.6 eV) respectively, which are consistent with the Au^0 state [18,24,47], indicating the existence of AuNPs in the composite. The C 1s peak is also detected at a binding energy of 284.5 eV, which is assigned to the C component of GNSs (Fig. 2(c)). The C 1s XPS spectrum of GNS/PEI/AuNP composite shows a significant decrease of signals at ca. 286.6 and 288.1 eV, which indicates the loss of C–O and C=O functionalities [18,19,46]. An exclusive single peak at 401.3 eV (Fig. 2(a)) is attributed to the nitrogen peak of imino-groups in PEI functionalized GNSs, which confirms the presence of PEI in the GNS/AuNP composite. It is also attributed to the formation of new C–N bonds between epoxy groups of GONS and free N groups of PEI [48]. These results

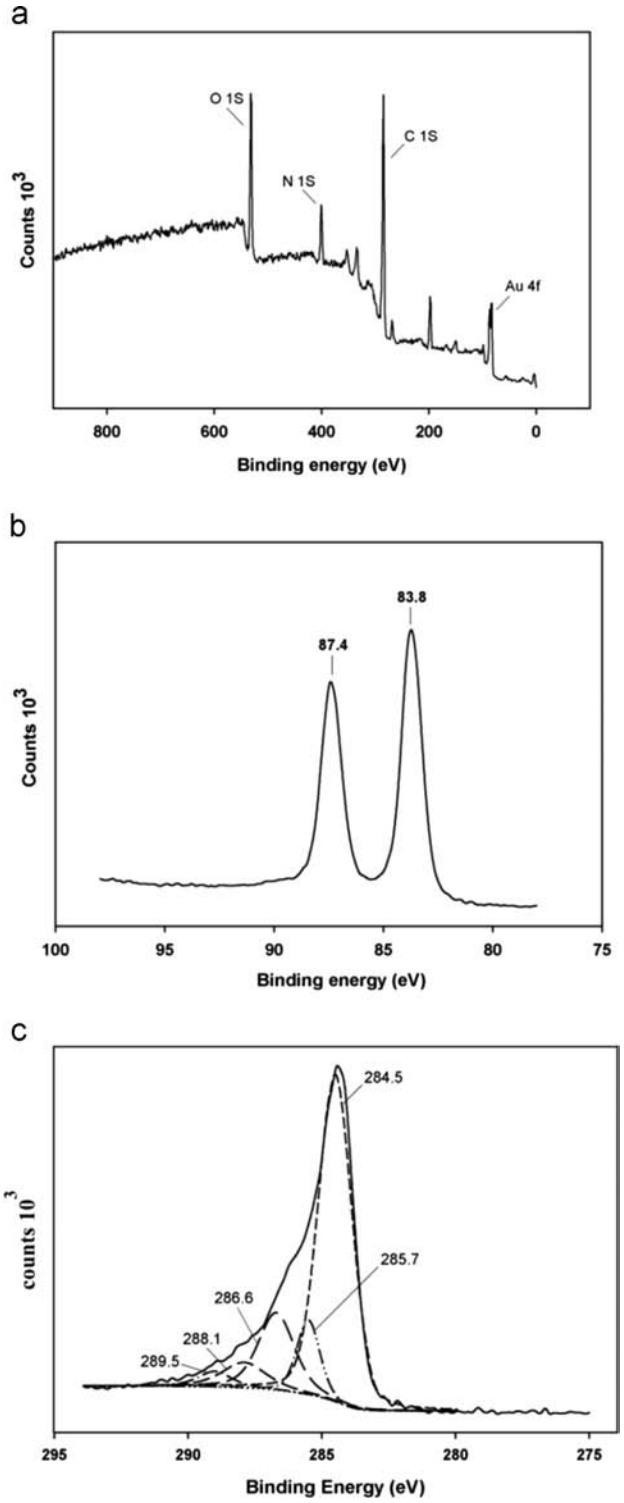

Fig. 2. (a) XPS spectrum (wide scan) of GNS/PEI/AuNP composite, (b) high resolution XPS spectrum of Au 4f of the as-prepared GNS/PEI/AuNP composite and (c) C 1s XPS spectra of GNS/PEI/AuNP composite.

suggest that GNS has been functionalized well by PEI with free NH_2 groups.

Fig. 3 displays the powder XRD patterns of the original graphite, GONSs and GNSs/PEI/AuNPs. The diffraction peaks at 2θ angles of 26.5 (d=3.4 Å) and 54.5 in the p-XRD pattern of graphite (Fig. 3(a)) can be assigned to hexagonal crystalline graphite [46]. As shown in the p-XRD pattern of GONSs (Fig. 3(b)), the disappearance of the native graphite position peak at about 26.5° and appearance of

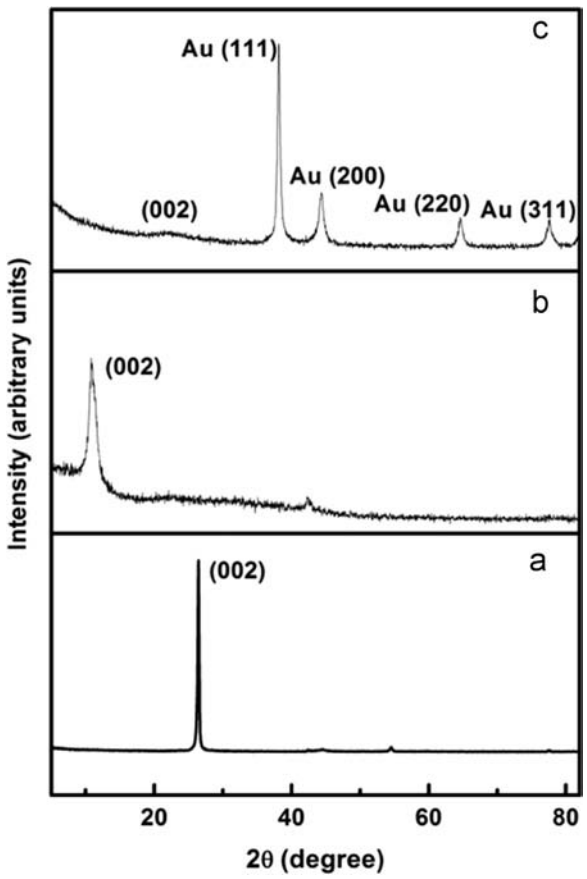

Fig. 3. p-XRD patterns of (a) graphite, (b) GONSs and (c) GNS/PEI/AuNP composite.

characteristic diffraction peak (002) at 10.6° (corresponding to interlayer spacing of 8.5 Å) reveals the successful oxidation of graphite [46]. The broad graphitic reflection in the p-XRD pattern of GNSs/PEI/AuNP composite (Fig. 3(c)) indicates that the GNSs are very thin, and the diffraction peaks at 38.7° for Au(111), 44.5° for Au (200), 64.8° for Au(220) and 77.8° for Au(311) confirm that the Au precursor ($HAuCl_4$) has been reduced to Au^0 on the surface of PEI wrapped GNS [17].

3.3. HR-TEM and FE-SEM characterizations of GNS/PEI/AuNP composite

The attachment of high density AuNPs on the surface of PEI wrapped GNS is inferred from the TEM images (Fig. 4). Fig. 4 (a) shows the TEM image of the GONS prior to the microwave assisted chemical reduction for the GNS/PEI/AuNP composite preparation. It can be seen that the GONS have large, smooth and transparent shaded planar surface. Fig. 4(c and d) shows the images of high density AuNPs attached on the PEI wrapped GNS. It is interesting to see that the high density AuNPs preferentially adhere to the surfaces of PEI wrapped GNS rather than to other regions that are devoid of GNS, due to the high affinity of AuNPs for the amino groups of the PEI and it can serve as primers for the adsorption of anionic $AuCl_4^-$ and function both as a reductant and a stabilizer which favor the reduction of $AuCl_4^-$ by facilitating electron transfer from the amine group of PEI to Au^{3+} along with the deoxygenation reaction of GONS to GNS under MWI [24,44]. Therefore, the AuNPs are selectively present on both the surfaces of GNS and are not found in the areas without GNS. A control experiment was also carried out without the addition of PEI into GONS to demonstrate the attachments of AuNPs on GNS by using only $NaBH_4$ in the absence of PEI under the same experimental

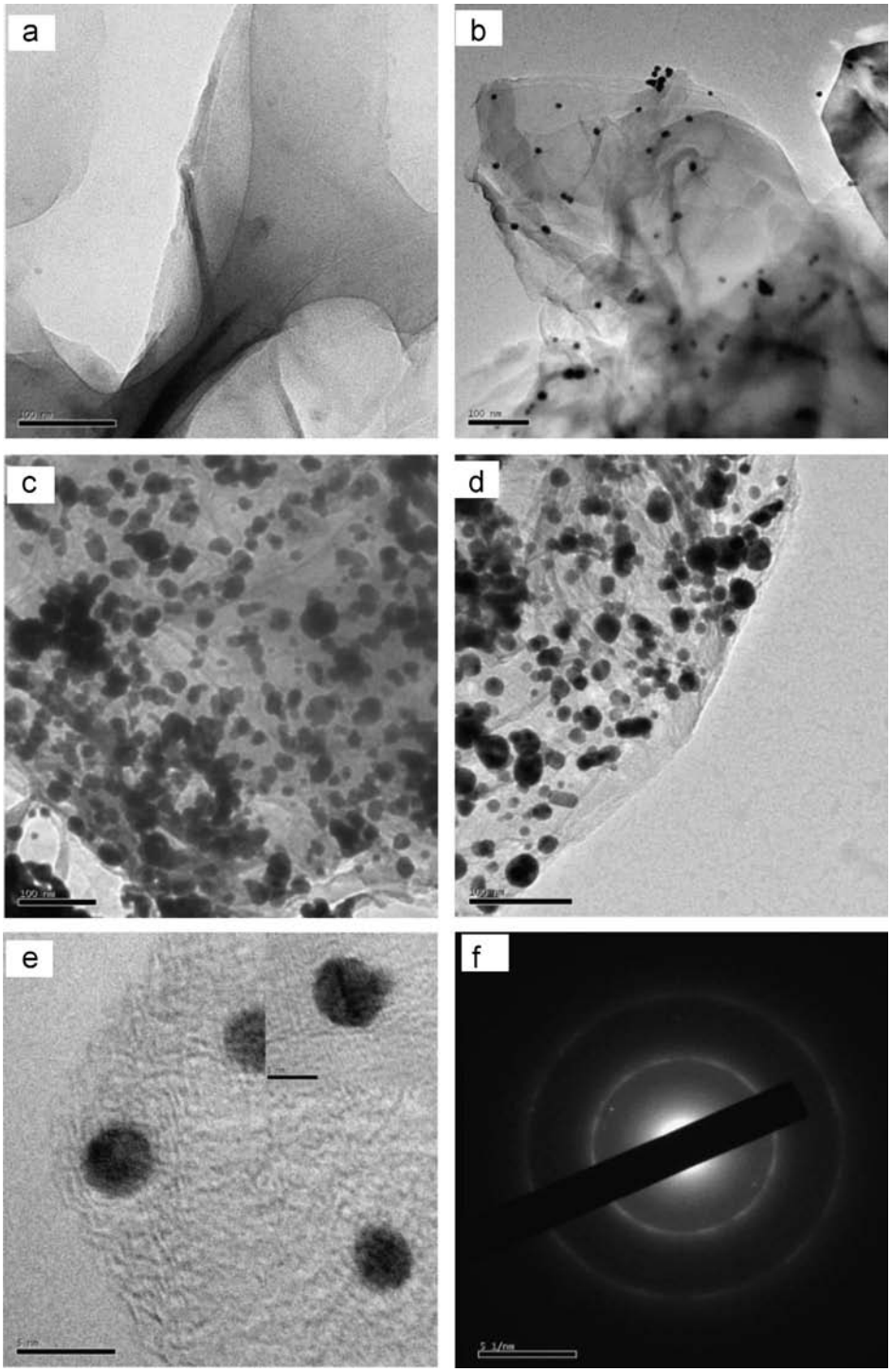

Fig. 4. (a) TEM image of GONSs, (b) TEM image of AuNPs attached GNSs in the absence of PEI, (c and d) TEM images of GNS/PEI/AuNP composite at 100 nm magnification, (e) HR-TEM image (at 5 nm magnification) of AuNPs on the single layer GNS, inset: lattice resolved HR-TEM image of the AuNPs on the single layer GNS, and (f) SAED pattern of GNS/PEI/AuNP composite.

conditions [44]. Fig. 4(b) (TEM image of AuNPs attached GNS in the absence of PEI) shows that the AuNPs were poorly dispersed on the surface of GNS [25]. It is also to be noted that AuNPs were scattered out of the sheets. We found that the incorporated crystalline AuNPs (Fig. 4(e), high resolution TEM (HR-TEM) images of GNS/PEI/AuNP composite) distributed uniformly on these single layer graphene sheets at high numbers. Furthermore, it allows us to distinguish the laminar lattice structure of the PEI wrapped GNSs and incorporated crystalline AuNPs with an interlayer distance of 0.20 nm (inset in Fig. 4(e)). The local selected area electron diffraction (SAED) pattern (Fig. 4(f)) reveals that the AuNPs [49] on the GNSs have a polycrystalline structure. The AuNPs have no tendency to aggregate at defects of the GNS surfaces.

FE-SEM was also used, in order to have a further insight into the coverage of AuNPs on PEI wrapped GNSs and to examine the morphology of the GNS/PEI/AuNP composite [17,46]. Fig. 5(a) shows typical FE-SEM images of GNS/PEI/AuNP composite. The AuNPs with an average diameter of 3 mm were decorated densely on the crumpled thin layer of PEI wrapped GNS (Fig. 5(b and c)). It is ascribed

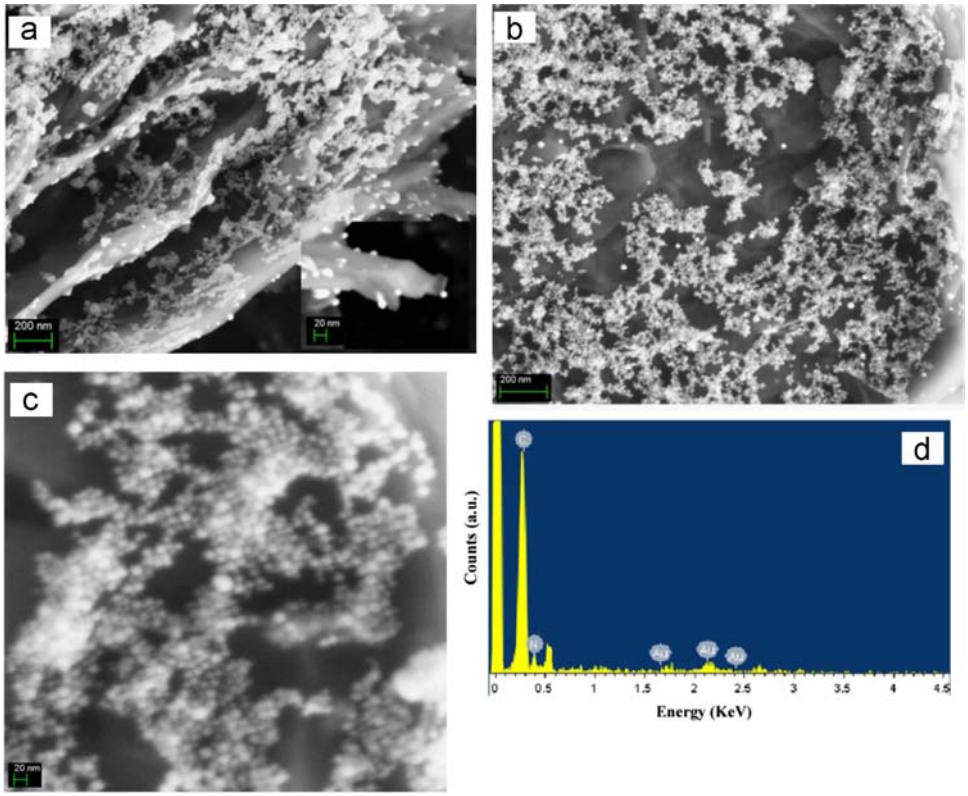

Fig. 5. (a and b) FE-SEM images of GNS/PEI/AuNP composite at 200 nm magnification, (c) FE-SEM image of GNS/PEI/AuNP composite at 20 nm magnification and (d) FE-SEM-EDX of GNS/PEI/AuNP composite.

that the presence of PEI showed greater the nucleation sites available for AuNPs on the GNS. Moreover, SEM-EDX of GNSs/AuNPs (Fig. 5(d)) also clearly demonstrates the presence of nitrogen peak and gold peaks which confirms the PEI functionalization on the GNSs. Therefore, FE-SEM studies demonstrate that this simple synthetic method opens up a new route for the fabrication of GNS/PEI/AuNP composite. Moreover, the controlled coating of AuNPs on GNSs favors the investigation of the electronic properties which would lead to the exploration of new types of electronic devices.

3.4. Thermal studies of the prepared composite

TGA was used to analyze the presence of functional groups on the GNSs, to understand the details of their decomposition process and to know the thermal stability of the as-prepared GNS/PEI/AuNP composite by heating under argon atmosphere to 850 °C at the rate of 10 °C/min (Fig. 6). GONSs are thermally unstable, and mass loss started below 100 °C which is attributed to the pyrolysis of labile oxygen-containing groups such as –OH, COOH, etc., and mass loss was rapid at 160 °C [50]. The lower starting temperature for rapid mass loss reported here (160 °C vs. 250 °C) reflects the higher defect density present in the GONSs sample (Fig. 6(a)) [50]. The GNS/PEI/AuNP composite (Fig. 6(b)) shows a less gradual weight loss, which is due to the absence of the epoxy and carboxylic functional groups of GNSs. The defunctionalization of the GNSs and decomposition of PEI are estimated to occur between 200 and 800 °C; it is noted that slow gradual weight loss occurs at lower temperatures ranging from 200 to 500 °C, which is entirely due to the removal of the wrapped PEI layer from the GNSs [45,50]. This confirms the wrapping of PEI on the surface of the GNSs.

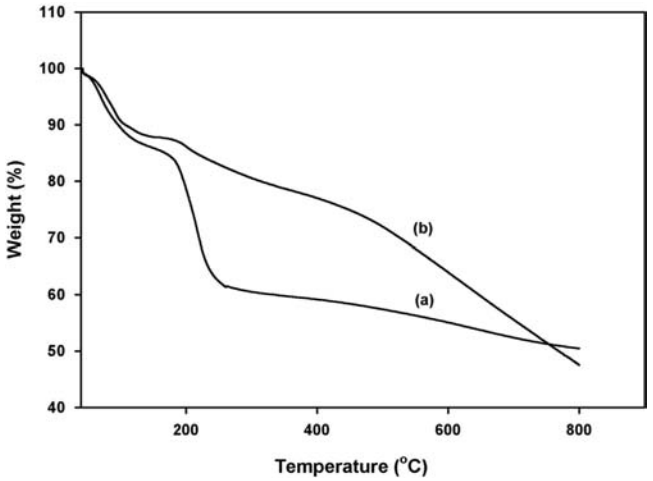

Fig. 6. TGA curves of the GONSs (a) and GNS/PEI/AuNP composite (b).

3.5. Electrochemical performance of the prepared GNS/PEI/AuNP composite

To elucidate the electrochemical behavior of the prepared GNS/PEI/AuNP composite, cyclic voltammograms (CV) was performed in PBS (pH 7) (Fig. 7(A)) at the potential range between −0.4 V and +1.2 V. A sharp cathodic peak was observed at the potential of +0.58 V which is attributed for the cathodic reduction of Au^{3+}, whereas a small anodic peak was observed at the potential of +1.00 V which is ascribed for the oxidation of Au nanoparticles consistent with the characteristic voltammogram behavior of Au nanoparticles [51]. In addition to that, a hydrogen adsorption desorption peak was also appeared at the potential of

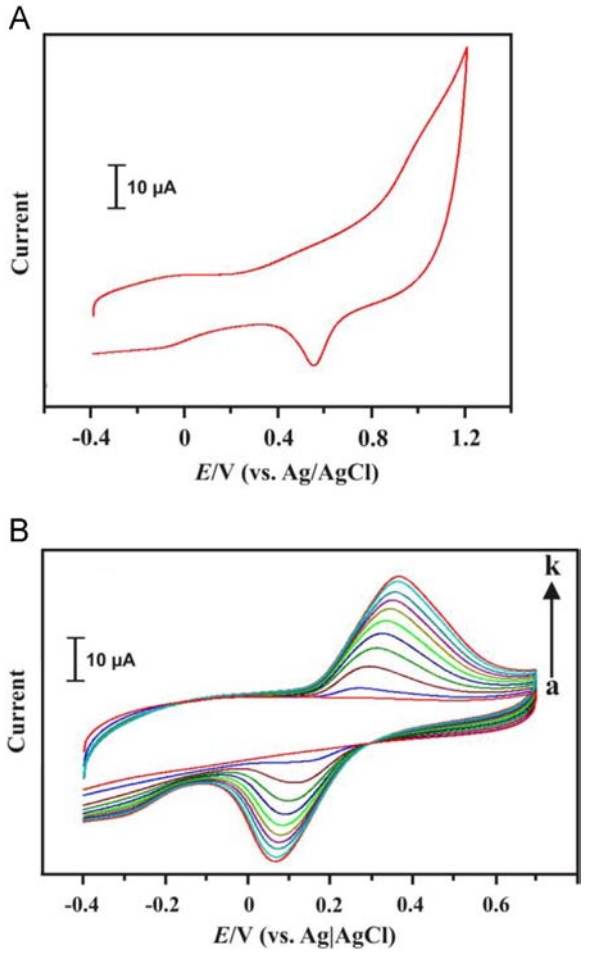

Fig. 7. (A) Cyclic voltammograms obtained at GNS/PEI/AuNP composite modified GCE in deoxygenated PBS (pH 7) at the scan rate of 50 mV s^{-1}. (B) Cyclic voltammograms obtained at GNS/PEI/AuNP composite modified GCE in the absence of DA (a) and in the presence of DA with the concentration ranging from 10 μM to 100 μM (b–k) in deoxygenated PBS (pH 7) at the scan rate of 50 mV s^{-1}.

−0.23 V. Fig. 7(B) shows the CVs of GNS/PEI/AuNP composite modified GCE in the absence (a) and presence of various concentrations of DA ranging from 10 μM to 100 μM (b–k) in deoxygenated PBS (pH 7) at the scan rate of 50 mV s^{-1}. A well defined anodic quasi-reversible peaks at the formal potential ($E^{o\prime}$) of +0.202 V have been observed upon 10 μM addition of DA ascribed to the redox reaction of DA at the modified electrode. The peak to peak separation value (ΔE_p) has been calculated to be +0.10 V. Here the anodic peak is attributed to the oxidation of DA to o-dopaminequinone and the cathodic peak is due to the reduction of dopaminequinone back to dopamine [27]. Both the anodic peak currents and cathodic peak currents linearly increase upon further addition of DA indicating the good electrocatalytic ability of the modified electrode towards electrocatalysis of DA. This must be ascribed to the excellent synergy between exceptional properties of graphene (large surface area, high conductivity, and presence of large amounts of edge plane sites) and gold nanoparticles (good electrocatalyst).

3.6. Determination of DA by differential pulse voltammetry (DPV)

Fig. 8(A) shows the DPVs obtained at GNS/PEI/AuNP composite modified GCE for the addition of various concentrations of DA (2–20 μM, curves a–k) in PBS (pH 7). When 1 μM of DA was added, a sharp anodic peak has been obtained at the potential of +0.18 V attributed to the electro-oxidation of DA at the modified electrode.

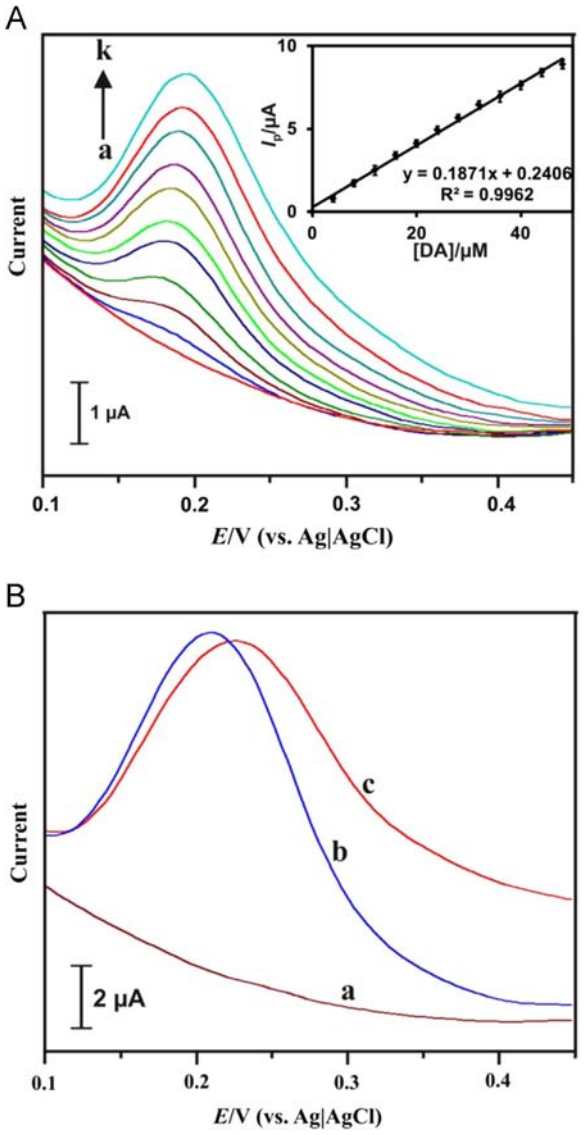

Fig. 8. (A) DPVs recorded at GNS/PEI/AuNP composite film modified GCE without DA (a) and with each addition of 2 μM DA (b–k; 2–20 μM) in PBS of pH 7 at the scan rate of 50 mV s^{-1}. Inset plot shows the linear dependence of I_{pa} vs. [DA]. (B) DPVs recorded at GNS/PEI/AuNPs composite film modified GCE without DA (a), with DA of 20 μM (b) and with a mixture of DA of 20 μM and AA of 2 mM (c).

Besides, the anodic peak current of DA linearly increases with further increase of DA concentrations from 2 to 20 μM (each addition of 2 μM). A linear calibration plot was made between the concentrations of DA and peak currents (Inset to Fig. 8(A)), and the respective linear regression equation can be expressed as $I_p/\mu A = 0.1871[DA]/\mu M + 0.2406$. It is evident from the plot that the fabricated sensor offered wide linear range from 2 to 48 μM with the sensitivity of 2.64 μA μM^{-1} cm^{-2}. Detection limit of the sensor was calculated to be 0.2 μM. The important electroanalytical parameters of the GNS/PEI/AuNP composite modified electrode was compared with other reported modified electrodes (Table 1). It is evident from Table 1 that the proposed sensor exhibited quite comparable electroanalytical performances with the previous reports revealing the ability of the sensor towards sensitive determination of DA. The excellent electrocatalytic ability of the modified electrode could be ascribed to the outstanding properties of graphene and decorated small sized AuNPs.

Interference study has been carried out to find the selectivity of the sensor towards common interference AA. Fig. 8(B) shows the

Table 1
Comparison of electroanalytical parameters for the determination of dopamine at GNS/PEI/AuNP composite modified electrode with other reported modified electrodes.

Electrode	Method	Sensitivity	Linear range/μM	[a]LOD/μM	Ref.
Graphene	[b]DPV	[c]NA	4–100	2.6	[29]
PEDOT/Pd composite	DPV	NA	0.5–1.0	0.5	[35]
Chitosan–graphene	DPV	NA	1.0–24	1.0	[38]
[d]Pt/PEDOT/PDA	Amperometry	0.74 μA μM^{-1}	1.5–50	0.65	[54]
[e]GE/Au/GE/CFE	DPV	NA	0.59–43.95	0.59	[55]
[f]$K_2UO_2[Fe(CN)_6]$/Pd–Al electrode	Amperometry	NA	1–50	0.41	[56]
Polypyrrole doped sulfonated β-cyclodextrins	Amperometry	0.89 μA μM^{-1}	NA	3.2	[57]
GNS/PEI/AuNP	DPV	2.64 μA μM^{-1} cm^{-2}	2–48	0.2	This work

[a] LOD – Limit of detection.
[b] DPV – Differential pulse voltammetry.
[c] NA – Not available.
[d] Pt/PEDOT/PDA – Platinum electrode/poly(3,4-ethylenedioxythiophene)/polydopamine hybrid film.
[e] GE/Au/GE/CFE – Layer-by-layer assembly of graphene sheets (GE) and gold nanoparticles modified carbon fiber electrode (CFE).
[f] $K_2UO_2[Fe(CN)_6]$ – Uranalyl hexacyanoferrates.

DPVs recorded at GNS/PEI/AuNP composite modified GCE in the absence (a) and presence of 20 μM DA (b) and mixture of 20 μM DA and 2 mM AA (c). A sharp anodic peak was observed at the potential of +0.20 V in the presence of 20 μM DA attributed to the electrocatalytic oxidation of DA as explained earlier. Afterwards, 2 mM of AA was added into this solution which does not show much interference to the response current of DA revealing the selective oxidation of DA in the presence of such a high concentration of AA. The selective elimination of the AA signal at the GNS/PEI/AuNP composite modified electrode can be explained by the following facts: (1) the incorporated negatively charged nafion in the composite film efficiently repels and blocks the negatively charged AA and selectively allows the movement of cationic DA for the electrocatalysis at the modified electrode surface [27], (2) π–π stacking interaction between graphene and phenyl moiety of DA is possible and which can assist the electron transfer and selectively attract DA for the electrocatalysis, whereas AA does not have any phenolic moiety to interact with graphene and therefore its detection at the modified electrode has been suppressed [52], (3) the presence of anionic AuNPs and GNSs makes the electrode negatively charged which finds a way for the electrostatic interaction with cationic DA, whereas the negatively charged surface of modified electrode repels the negatively charged AA. These three factors are the plausible reasons for the high selectivity of the modified electrode towards DA in the presence of AA.

3.7. Determination of DA by amperometry

Fig. 9(A) displays the amperogram obtained at GNS/PEI/AuNP composite film modified rotating disc GCE (rotation speed of 1500 rpm) upon sequential injection of 1 μM DA into PBS (pH 7) at regular intervals of 50 s. The applied potential of the electrode was hold at +0.20 V. Each addition of DA produces well defined and stable amperometric responses. The steady state current was reached within 5 s of aliquots of DA addition. The amperometric response currents increase linearly upon further addition of DA. A calibration plot was made between the concentrations of DA and peak currents which exhibited a good linear relationship (inset to Fig. 9(A)). The linear regression equation can be expressed as, $I/\mu A = 0.0452\,[DA]/\mu M + 1.1221$. The linear range of the sensor is ranging between 1 and 83 μM and the sensitivity was 0.2 μA μM^{-1} cm^{-2}. The limit of detection (LOD) and limit of quantification (LOQ) were 0.2 μM and 0.7 μM, using the equations, $LOD = 3S_b/S$ and $LOQ = 10S_b/S$ respectively, where S_b is the standard deviation of the blank signal and S is the sensitivity [53].

We explored the selectivity of the GNS/PEI/AuNP composite modified rotating disc GCE towards DA in the presence of common interference AA (Fig. 9(B)). The applied potential of the electrode

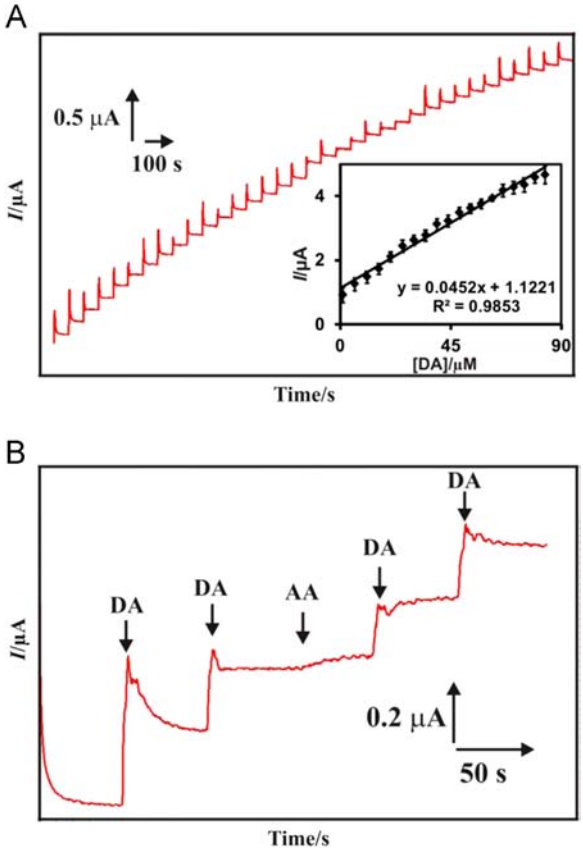

Fig. 9. (A) Amperometric *i–t* response obtained at GNS/PEI/AuNP composite film modified rotating disc GCE upon successive additions of 1 μM DA into PBS of pH 7. Rotation rate: 1500 rpm; $E_{app} = +0.20$ V. Inset is the linear calibration plot of response current vs. [DA]. (B) Amperometric *i–t* response at GNS/PEI/AuNP composite film modified rotating disc GCE towards 1 μM of DA and 5 mM of AA.

was hold at +0.20 V, while the rotation speed was kept at 1500 rpm. The modified electrode exhibited well defined amperometric response towards addition of 1 μM DA, whereas no noteworthy response was observed for the addition of 5 mM AA. However, notable amperometric response was observed upon the addition of 1 μM DA into the same PBS coexisted with AA. Accordingly, GNS/PEI/AuNP composite film modified GCE selectively gives access to DA only and denied the access to AA revealing the excellent selectivity of the modified electrode. As explained in the DPV section, electrostatic repulsion between negatively charged electrode surface and negatively charged AA might be the plausible reason for the repulsion of AA. Thus,

Table 2
Determination of DA in human urine sample at GNS/PEI/AuNP composite modified electrode.

Real sample	Sample	Added/μM	Found/μM	Recovery/%	[a]RSD/%
Urine sample	1	10	9.8	97.9	3.7
	2	20	19.7	98.7	2.9

[a] Relative standard deviation (RSD) of 3 independent measurements.

amperometric experimental results proved that the proposed sensor can be used for the sensitive and selective determination of DA even in the presence of high concentration of AA.

3.8. Real sample analysis

The practical feasibility of the developed sensor was assessed for the determination of DA in human urine sample. Human urine sample was collected from a healthy man and diluted it with PBS (pH 7) to the ratio of 1:50 (v/v). The diluted urine sample was stored at the temperature of 4 °C until the analysis time. The experimental results showed that the analyzed urine sample was free of DA. Recoveries and relative standard deviation (RSD) of DA for the real sample was evaluated at two different spiked concentration levels (10 and 20 μM) under the similar experimental conditions and the results were listed in Table 2. As can be seen from Table 2, the developed sensor showed the recoveries ranged from 97.9 to 98.7% with the RSDs between 2.9 and 3.7%. These experimental results clearly demonstrated that the recoveries and RSDs of the developed sensor for the determination of DA in the spiked human urine samples were deemed acceptable and thus proven the promising practicality of the proposed sensor towards real sample analysis.

3.9. Stability, repeatability and reproducibility studies

In order to examine the stability, the GNS/PEI/AuNP/GCE was stored in PBS (pH 7) solution at 4 °C and its electrocatalytic response towards 100 μM of DA was monitored for seven days at each 24 h time interval. The presented electrode retained 96.38% of its initial electrocatalytic response even after one week of its storage validating period which reveals that the presented electrode possessed acceptable storage stability. To investigate the repeatability and reproducibility of the presented sensor, CVs were recorded in PBS (pH 7) at the scan rate of 50 mV s^{-1} in the presence of 100 μM of DA. The developed sensor exhibited RSD of 2.19% for 10 repeated measurements in a single modified electrode which showed appreciable repeatability of the developed sensor. In addition, the sensor exhibited RSD of 3.79% for 5 individual measurements carried out in five different modified electrodes which also showed the satisfactory reproducibility of the sensor towards determination of DA.

4. Conclusions

An efficient and practical method for preparing high density AuNPs attached on PEI wrapped GNS surfaces (GNS/PEI/AuNP composite) was developed. This simple synthetic route involves a mild MWI process, which involves one step simultaneous chemical reduction of $HAuCl_4$ and GONS for the formation of AuNPs decorated PEI wrapped GNSs composite. Characterization results reveal that the thin, smooth and transparent planar GNS were decorated with well-dispersed and uniform spherical AuNPs being attached on the external surfaces of PEI wrapped GNS. The prepared GNS/PEI/AuNP composite exhibited excellent electrocatalytic behavior towards selective determination of DA. The composite film modified electrode selectively detects DA even in the presence of high concentration of AA via both amperometry and DPV. Acceptable recoveries and RSDs were achieved in the real samples analysis which revealed the promising practicality of the presented sensor. Although only AuNPs were investigated here, this simple and rapid NP attachment technique could be easily extended to other types of metallic and bimetallic NPs that can be decorated on the GNS in order to create novel polymer supported few layered 2-D graphene nanocatalysts for their potential applications in fields such as chemical sensors and catalysis.

Acknowledgment

The authors thank the National Science Council of Taiwan under grants of NSC-98-2113-M-005-016-MY3 and NSC-101-2811-M-005-014, and National Chung Hsing University for financial supports.

References

[1] K.S. Novoselov, D. Jiang, F. Schedin, T.J. Booth, V.V. Khotkevich, S.V. Morozov, A.K. Geim, Proc. Natl. Acad. Sci. USA 102 (2005) 10451–10453.
[2] A.K. Geim, K.S. Novoselov, Nat. Mater. 6 (2007) 183–191.
[3] S. Stankovich, D.A. Dikin, G.H.B. Dommett, K.A. Kohlhaas, E.J. Zimney, E.A. Stach, R.D. Piner, S.T. Nguyen, R.S. Ruoff, Nature 442 (2006) 282–286.
[4] V. Georgakilas, D. Gournisb, V. Tzitziosa, L. Pasquato, D.M. Guldie, M. Prato, J. Mater. Chem. 26 (2007) 2679–2694.
[5] S. Niyogi, E. Bekyarova, M.E. Itkis, J.L. McWilliams, M.A. Hamon, R.C. Haddon, J. Am. Chem. Soc. 128 (2006) 7720–7721.
[6] D.A. Dikin, S. Stankovich, E.J. Zimney, R.D. Piner, G.H.B. Dommett, G. Evmenenko, S.T. Nguyen, R.S. Ruoff, Nature 448 (2007) 457–460.
[7] D. Li, M.B. Muller, S. Gilje, R.B. Kaner, G.G. Wallace, Nat. Nanotechnol. 3 (2007) 101–105.
[8] G. Eda, G. Fanchini, M. Chhowalla, Nat. Nanotechnol. 3 (2008) 270–274.
[9] M.J. McAllister, J.L. Li, D.H. Adamson, H.C. Schniepp, A.A. Abdala, J. Liu, M. Herrera-Alonso, D.L. Milius, R. Car, R.K. Prud'homme, I.A. Aksay, Chem. Mater. 19 (2007) 4396–4404.
[10] G. Wang, J. Yang, J. Park, X. Gou, B. Wang, H. Liu, J. Yao, J. Phys. Chem. C 112 (2008) 8192–8195.
[11] T.T. Ramanathan, A.A. Abdala, S. Stankovich, D.A. Dikin, H.M. Alonso, R.D. Piner, Nat. Nanotechnol. 3 (2008) 327–331.
[12] S. Stankovich, R.D. Piner, X.Q. Chen, N.Q. Wu, S.T. Nguyen, R.S. Ruoff, J. Mater. Chem. 16 (2006) 155–158.
[13] X.K. Lu, M.F. Yu, H. Huang, R.S. Ruoff, Nanotechnology 10 (1999) 269–272.
[14] A.P. Yu, P. Ramesh, M.E. Itkis, E. Bekyarova, R.C. Haddon, J. Phys. Chem. C 111 (2007) 7565–7569.
[15] Y. Gan, L. Sun, F. Banhart, Small 4 (2008) 587–591.
[16] R. Muszynski, B. Seger, P.V. Kamat, J. Phys. Chem. C 112 (2008) 5263–5266.
[17] C. Xu, X. Wang, J. Zhu, J. Phys. Chem. C 112 (2008) 19841–19845.
[18] F. Li, H. Yang, C. Shan, Q. Zhang, D. Han, A. Ivaska, L. Niu, J. Mater. Chem. 19 (2009) 4022–4025.
[19] S. Park, A.D. Dikin, T.S. Nguyen, S.R. Ruoff, J. Phys. Chem. C 113 (2009) 15801–15804.
[20] S.B. Kong, W.H. Yoo, T.H. Jung, Langmuir 25 (2009) 11008–11013.
[21] Y. Tian, J.G. Park, Q. Cheng, Z. Liang, C. Zhang, B. Wang, Nanotechnology 20 (2009) 335601–335606.
[22] Y.Y. Ou, M.H. Huang, J. Phys. Chem. B 110 (2006) 2031–2036.
[23] E. Munoz, D.S. Suh, S. Collins, M. Selvidge, A.B. Dalton, B.G. Kim, J.M. Razal, G. Ussery, A.G. Rinzler, M.T. Martınez, R.H. Baughman, Adv. Mater. 17 (2005) 1064–1069.
[24] X. Hu, T. Wang, X. Qu, S. Dong, J. Phys. Chem. B 110 (2006) 853–857.
[25] H.M.A. Hassan, V. Abdelsayed, A.E.R.S. Khder, K.M. AbouZeid, J. Terner, M.S. EI-Shall, J. Mater. Chem. 19 (2009) 3832–3837.
[26] C.M. Shen, C. Hui, T.Z. Yang, C.W. Xiao, J.F. Tian, L.H. Bao, S.T. Chen, H.Ding Gao, J. Chem. Mater. 20 (2008) 6939–6944.
[27] R. Thangamuthu, Y.-C. Wu, S.-M. Chen, Electroanalysis 21 (2009) 994–998.
[28] A. Balamurugan, S.-M. Chen, Anal. Chim. Acta 596 (2007) 92–98.
[29] Y.-R. Kim, S. Bong, Y.-J. Kang, Y. Yang, R.K. Mahajan, J.S. Kim, H. Kim, Biosens. Bioelectron. 25 (2010) 2366–2369.
[30] S.-M. Chen, J.-Y. Chen, R. Thangamuthu, Electroanalysis 19 (2007) 1531–1538.
[31] Y. Zhao, Y. Gao, D. Zhan, H. Liu, Q. Zhao, Y. Kou, Y. Shao, M. Li, Q. Zhuang, Z. Zhu, Talanta 66 (2005) 51–57.
[32] C. Deng, J. Chen, M. Wang, C. Xiao, Z. Nie, S. Yao, Biosens. Bioelectron. 24 (2009) 2091–2094.
[33] Z. Wang, J. Xia, L. Zhu, X. Chen, F. Zhang, S. Yao, Y. Li, Y. Xia, Electroanalysis 23 (2011) 2463–2471.
[34] P. Si, H. Chen, P. Kannan, D.-H. Kim, Analyst 136 (2011) 5134–5138.

[35] S. Harish, J. Mathiyarasu, K.L.N. Phani, V. Yegnaraman, J. Appl. Electrochem. 38 (2008) 1583–1588.
[36] L. Wu, L. Feng, J. Ren, X. Qu, Biosens. Bioelectron. 34 (2012) 57–62.
[37] S. Yang, Y. Yin, G. Li, R. Yang, J. Li, L. Qu, Sens. Actuators, B 178 (2013) 217–221.
[38] D. Han, T. Han, C. Shan, A. Ivaska, L. Niu, Electroanalysis 22 (2010) 2001–2008.
[39] J. Li, J. Yang, Z. Yang, Y. Li, S. Yu, Q. Xu, X. Hu, Anal. Methods 4 (2012) 1725–1728.
[40] W.S. Hummers, R.E. Offeman, J. Am. Chem. Soc. 80 (1958) 1339.
[41] M.C. Wei, J.F. Jen, J. Chromatogr. A 1012 (2003) 111–118.
[42] A. Carrillo, J.A. Swartz, J.M. Gamba, R.S. Kane, Nano Lett. 3 (2003) 1437–1440.
[43] N.A. Kumar, A. Bund, B.G. Cho, K.T. Lim, Y.T. Jeong, Nanotechnology 20 (2009) 225608.
[44] X. Hu, T. Wang, L. Wang, S. Guo, S. Dong, Langmuir 23 (2007) 6352–6357.
[45] H. Hu, Y. Ni, S.K. Mandal, V. Montana, B. Zhao, R.C. Haddon, V. Parpura, J. Phys. Chem. B 109 (2005) 4285–4289.
[46] V.A. Murugan, T. Muraliganth, A. Manthiram, Chem. Mater. 21 (2009) 5004–5006.
[47] C. Shana, H. Yanga, D. Hana, Q. Zhanga, A. Ivaska, L. Niua, Biosens. Bioelectron. 25 (2010) 1070–1074.
[48] E.P. Dillon, C.A. Crouse, A.R. Barron, Am. Chem. Soc. Nano 2 (2008) 156–164.
[49] X. Hou, L. Wang, F. Zhou, F. Wang, Carbon 47 (2009) 1209–1213.
[50] G. Goncalves, P.A.A.P. Marques, C.M. Granadeiro, H.I.S. Nogueira, M.K. Singh, J. Gracio, Chem. Mater. 21 (2009) 4796–4802.
[51] C.-Y. Cheng, S. Thiagarajan, S.-M. Chen, Int. J. Electrochem. Sci. 6 (2011) 1331–1341.
[52] Y. Wang, Y. Li, L. Tang, J. Lu, J. Li, Electrochem. Commun. 11 (2009) 889–892.
[53] A. Radoi, D. Compagnone, E. Devic, G. Palleschi, Sens. Actuators, B 121 (2007) 501–506.
[54] R. Salgado, R.d. Rio, M.A.d. Valle, F. Armijo, J. Electroanal. Chem. 704 (2013) 130–136.
[55] J. Du, R. Yue, F. Ren, Z. Yao, F. Jiang, P. Yang, Y. Du, Gold Bull. 46 (2013) 137–144.
[56] M.H.P. Azar, H. Dastangoo, R.F.B. baj, Biosens. Bioelectron. 25 (2010) 1481–1486.
[57] C.C. Harley, A.D. Rooney, C.B. Breslin, Sens. Actuators, B 150 (2010) 498–504.